

# Task Aware Modulation using Representation Learning for Upsaling of Terrestrial Carbon Fluxes

Aleksei Rozanov<sup>1\*</sup>, Arvind Renganathan<sup>1\*</sup>, Vipin Kumar<sup>1</sup>

<sup>1</sup>University of Minnesota, Twin Cities  
{rozan012, renga016, kumar001}@umn.edu

## Abstract

Accurately upscaling terrestrial carbon fluxes is central to estimating the global carbon budget, yet remains challenging due to the sparse and regionally biased distribution of ground measurements. Existing data-driven upscaling products often fail to generalize beyond observed domains, leading to systematic regional biases and high predictive uncertainty. We introduce Task-Aware Modulation with Representation Learning (TAM-RL), a framework that couples spatio-temporal representation learning with knowledge-guided encoder-decoder architecture and loss function derived from the carbon balance equation. Across 150+ flux tower sites representing diverse biomes and climate regimes, TAM-RL improves predictive performance relative to existing state-of-the-art datasets, reducing RMSE by 8–9.6% and increasing explained variance ( $R^2$ ) from 19.4% to 43.8%, depending on the target flux. These results demonstrate that integrating physically grounded constraints with adaptive representation learning can substantially enhance the robustness and transferability of global carbon flux estimates.

## Introduction

Accurately quantifying the exchange of carbon dioxide between land and atmosphere is essential for understanding the global carbon balance and predicting climate feedbacks (Masson-Delmotte et al. 2021). Eddy covariance (EC) towers provide direct *in-situ* measurements of terrestrial carbon fluxes such as net ecosystem exchange (NEE), gross primary production (GPP), and ecosystem respiration (RECO). However, each tower observes only a small area (typically a few square kilometers), making global coverage infeasible. To address this limitation, large-scale networks such as FLUXNET (Baldocchi et al. 2001) and AmeriFlux (Novick et al. 2018) aggregate and distribute EC data from several hundred sites worldwide, with most located in North America and Europe (Fig. 1). While EC measurements provide high-fidelity flux estimates at individual sites, their coverage is insufficient to produce spatially continuous assessments of global carbon sequestration needed for climate policy, car-

bon accounting, and parameterization of Earth system models.

Yet, given this data, an upscaling task can be formulated as inferring a continuous flux field from ground-level data and gridded datasets using a non-linear estimator. Classical methods such as resampling and spatial interpolation (bilinear, spline, kriging) perform poorly because they ignore ecosystem context and temporal variability. In contrast, recent advances in representation learning have opened new opportunities for integrating satellite-based observations, which provide dense spatial coverage of vegetation and surface properties, and meteorological data to predict carbon fluxes at regional and global scales. Combining these complementary modalities enables data-driven models to infer fluxes in unobserved regions. Yet, despite impressive results, most ML-based upscaling frameworks remain domain-specific – trained and evaluated on limited sets of flux towers – and their generalization to unseen biomes and climates remains weak.

A key reason is that flux–feature relationships are highly context-dependent: the same satellite-derived vegetation index may indicate different physiological states under varying weather conditions. Furthermore, differences in data resolution, noise characteristics, and temporal coverage introduce covariate shifts that standard ML models cannot handle. As a result, current approaches often excel within known regions but fail when transferred globally.

To overcome these limitations, recent research emphasizes domain generalization and task-aware learning approaches that explicitly separate location-specific variability from generalizable ecosystem dynamics. By learning invariant representations that capture process-level dependencies rather than purely statistical correlations, such methods aim to produce models that scale robustly across ecosystems, climates, and temporal contexts.

Thus, here we propose applying the Task-Aware Modulation with Representation Learning (TAM-RL) framework (Renganathan et al. 2025) to the problem of upscaling of terrestrial carbon fluxes. The original TAM-RL approach combines an LSTM-based temporal encoder that captures location-specific attributes and produces a latent representation with a modulated decoder that generates the final predictions. Originally developed for few-shot learning, this framework has already demonstrated strong per-

\*These authors contributed equally.

This paper was accepted to the KGML Bridge at AAAI 2026 (non-archival).

Copyright © 2024, Association for the Advancement of Artificial Intelligence (www.aaai.org). All rights reserved.



Figure 1: Spatial distribution of the sites used in the current study where color represents climate type according to Köppen–Geiger climate classification (Cui et al. 2021). The sites are derived from the FLUXCOM, AmeriFlux, ICOS, and JapanFlux networks.

formance across several environmental modeling tasks. Our work makes the following novel contributions:

- We extend TAM-RL to the domain generalization setting, evaluating its ability to perform global carbon flux upscaling without site-specific fine-tuning, e.g. zero-shot;
- We design a knowledge-guided loss function incorporating the carbon balance equation ( $NEE = GPP - RECO$ ), quality-control weighting, and class balancing across ecosystem types;
- We demonstrate significant performance gains over current state-of-the-art analog, achieving an average RMSE reduction of 8–9.6% and an  $R^2$  increase of 19.4–43.8% across all ecosystem types.

Overall, our results show that TAM-RL effectively addresses the domain generalization challenge and outperforms classical tree-based models that depend on extensive manual feature engineering.

## Related Works

### Knowledge-Guided ML

Despite the widespread use of process-based models in Earth system science, their performance is often limited by structural biases, incomplete process representations, and high computational demands. As an alternative, data-driven machine learning (ML) approaches have gained substantial traction over the past decade, offering high efficiency during inference, flexibility in incorporating diverse input drivers, and the ability to learn rich feature representations – particularly when neural networks (NNs) are employed. However, purely data-driven methods tend to overfit and exhibit poor generalization in data-sparse setups. Knowledge-Guided Machine Learning (KGML) has emerged as a promising paradigm that combines the strengths of process-based and data-driven modeling, enabling faster convergence, improved physical consistency, and better generalization.

According to (Karpatne, Jia, and Kumar 2024), strategies for incorporating scientific knowledge into ML can be grouped into three main categories:

- (a) Modifying the learning algorithm, for instance by embedding domain constraints directly into the loss function;

- (b) Integrating scientific knowledge into the model architecture, such as by constraining intermediate layers or designing physics-informed structures;
- (c) Knowledge-guided weight initialization, for example through pre-training on outputs of physical or “surrogate” models.

Due to space constraints, we forgo a comprehensive review of related work. KGML has been widely explored across scientific domains, including chemistry (Ji and Deng 2021; Wu et al. 2023), physics (Cai et al. 2021; Ren et al. 2022), hydrology (Read et al. 2019; Xu and Valocchi 2015), and climate science (Liu et al. 2024), demonstrating its broad applicability for learning system dynamics, surrogate modeling, and prior-informed frameworks.

### Carbon Flux Upscaling

Carbon flux upscaling methods typically derive targets from EC networks and predict GPP, RECO, and/or NEE from remote sensing and meteorological inputs. The most prominent framework is FLUXCOM (Jung et al. 2020) and its successor FLUXCOM-X-BASE (Nelson et al. 2024), which uses XGBoost (Chen and Guestrin 2016) with MODIS and climate forcings at hourly,  $0.05^\circ$  resolution — we use it as our state-of-the-art baseline. Recent work has explored meta-learning (Nathaniel, Liu, and Gentine 2023), PFT-specialized mixture of experts (Yuan et al. 2025), and KGML approaches (Fan et al. 2025), but to our knowledge none has framed  $\text{CO}_2$  upscaling as a zero-shot regression transfer learning problem.

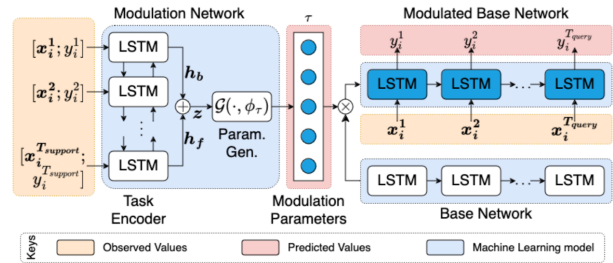


Figure 2: TAM-RL Architecture

## Methodology

### Dataset

Our dataset integrates eddy covariance (EC) fluxes, MODIS satellite observations, and ERA5-Land reanalysis data. Ground-truth fluxes are derived from 579 EC sites (2000–2023) across FLUXNET, AmeriFlux, ICOS (Rebmann et al. 2018), and JapanFlux (Ueyama et al. 2025), spanning all Köppen–Geiger climate classes (Fig. 1), following the ONEFlux standard (Pastorello et al. 2020) for daily GPP\_NT\_VUT\_USTAR50 (GPP) and NEE\_VUT\_USTAR50 (NEE) estimates with NEE\_VUT\_USTAR50\_QC used as a continuous quality flag ranging from 0 to 1. Vegetation properties come from MODIS, particularly MOD09GA (Vermeire and Wolfe 2015) and MCD12Q1 (Friedl and Sulla-Menashe 2019), at 500 m resolution, extracted over a

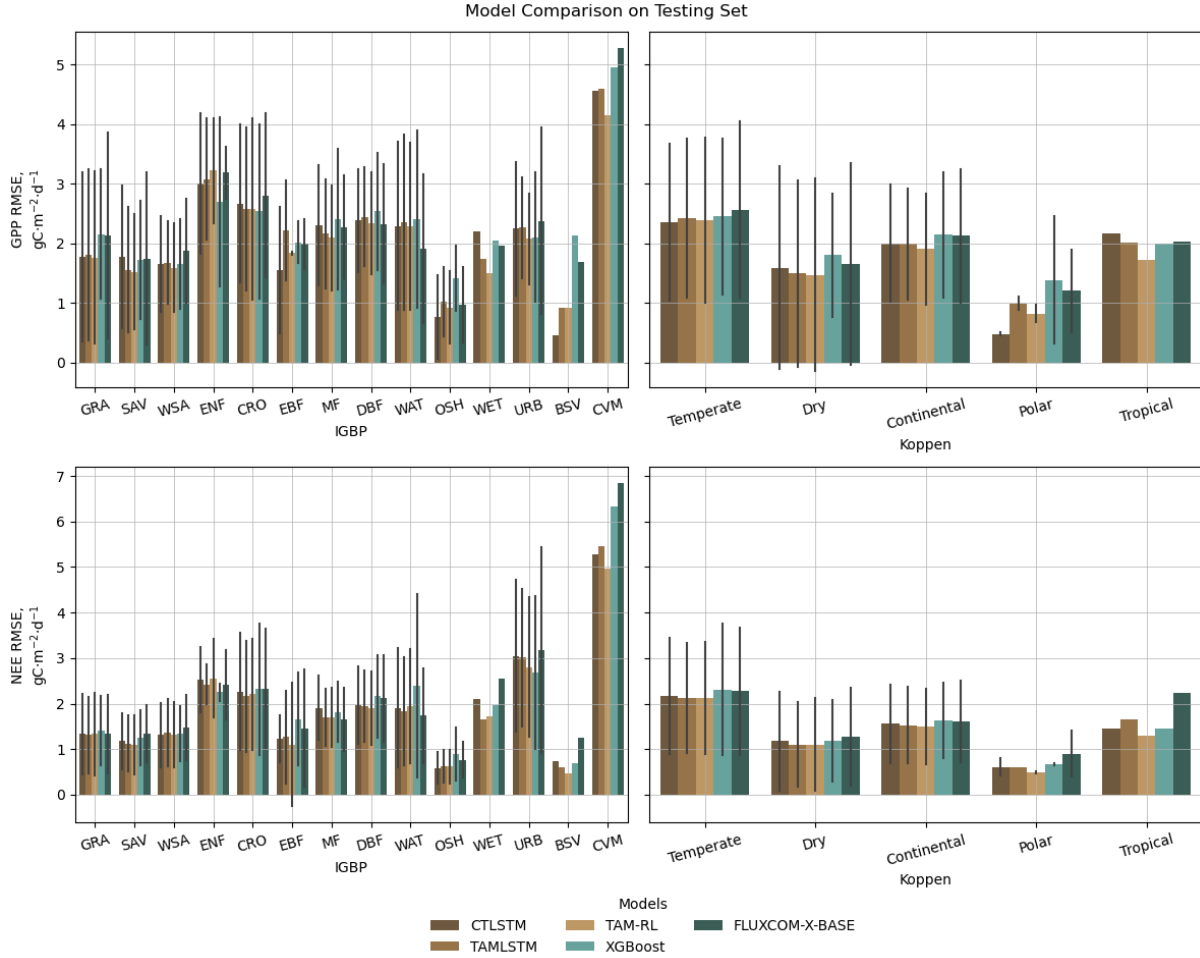


Figure 3: Barplots illustrating mean RMSE of CT-LSTM, TAMLSTL, TAM-RL, XGBoost and FLUXCOM-X-BASE aggregated by IGBP and Köppen climate types. The error bars are computed for classes with more than one site presenting them. NEE\_VUT\_USTAR50\_QC=1.

2 km  $\times$  2 km tower window via Google Earth Engine (Gorelick et al. 2017). Meteorological predictors are from ERA5-Land (Muñoz-Sabater et al. 2021) at 0.1° resolution. All inputs are harmonized to daily resolution with a 45-day sequence window and 15-day stride.

### Loss Function

We use a composite loss enforcing data quality, class balance, and physical consistency:

$$\mathcal{L} = \text{MSE} \cdot w_{qc} \cdot w_{igbp} \cdot w_{koppen} + \alpha \cdot L_{flux}, \quad \alpha = 0.1$$

where  $w_{qc}$  weights samples by their continuous NEE quality flag,  $w_{igbp}$  and  $w_{koppen}$  are inverse-frequency class weights countering spatial imbalance across ecosystem and climate types, and  $L_{flux}$  penalizes violations of  $\text{NEE} = \text{RECO} - \text{GPP}$ . GPP and RECO are clipped to non-negative values at inference.

### Task-Aware Modulation using Representation Learning

We leverage the TAM-RL framework (Fig. 2). The architecture consists of two main components:

- **Modulation network:** Composed of a BiLSTM-based task encoder  $\mathcal{E}$  and a modulation parameter generator  $G$ . The encoder captures temporal information and learns task-specific embeddings  $z_i$  representing the characteristics of each entity (site). These embeddings are then used by the MLP-based generator  $G$  to produce modulation parameters.
- **Forward model  $\mathcal{F}$ :** A standard LSTM decoder used for conditional generation of sequential responses given the driver data. During inference, the modulation network provides task-specific meta-initialization for  $F$ .

Modulation is a crucial component of TAM-RL, and is applied at two points: the input layer and the final hidden state, using Feature-wise Linear Modulation (FiLM):

$$x' = \gamma_1 \odot x + \beta_1,$$

$$h' = \gamma_2 \odot h + \beta_2,$$

where  $x'$  and  $h'$  is input and hidden state after modulation,  $x$  and  $h$  input and hidden state before modulation,  $\odot$  denotes element-wise multiplication, and  $\gamma_i, \beta_i$  are the learned modulation parameters.

Training occurs in two stages:

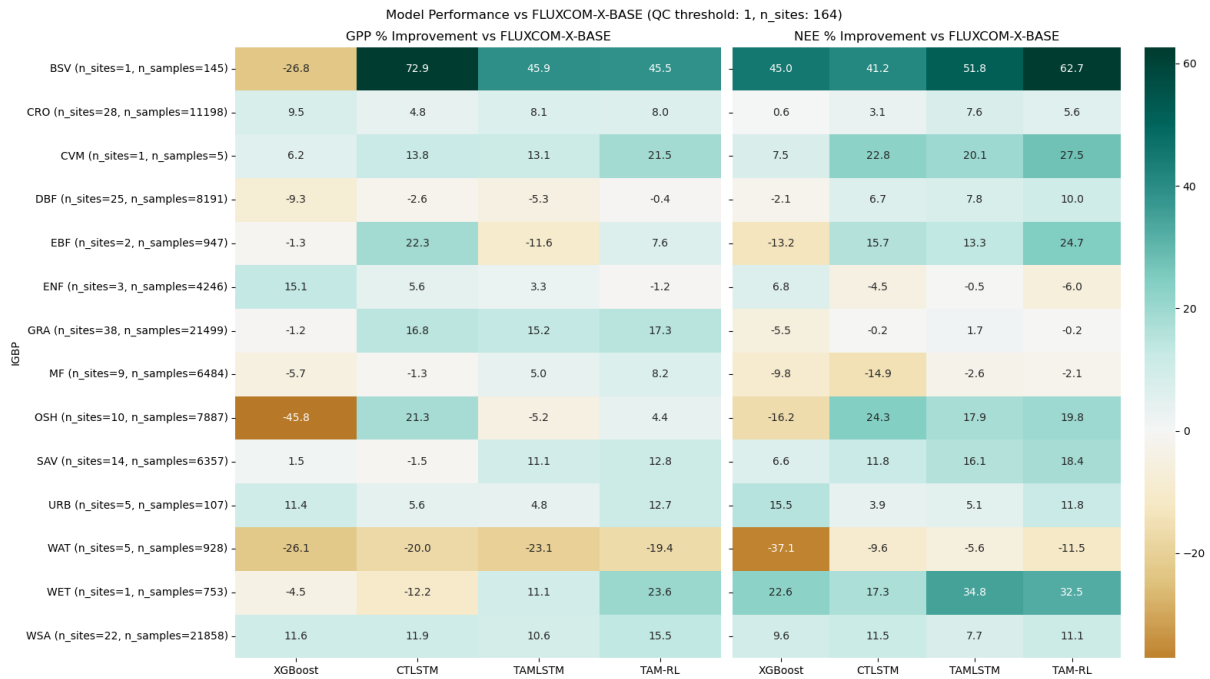


Figure 4: Relative RMSE heatmap of XGBoost, CT-LSTM, TAMLSTM, and TAM-RL derived in comparison to FLUXCOM-X-BASE with NEE\_VUT\_USTAR50\_QC=1.

- Pre-training:** Only the decoder network is trained without using any task-specific information. By initializing the model with these pre-trained weights, the decoder is provided with a robust foundation that has shared knowledge across the distribution for subsequent task-specific adaptation.
- Joint training:** For each task (carbon site), a small support set is used to compute the task embedding. The modulation network converts this embedding into parameters that adjust both the shared feature extractor and prediction head. A separate query set is passed to the adapted decoder, and gradients are backpropagated through both networks. This enables TAM-RL to learn how to modulate representations for new tasks using only a few examples, without test-time fine-tuning.

During inference, historical data for each site (e.g., 2001, 2011, 2021) serves as the support set to derive site context. The modulated base network then generates final predictions for each task.

## Results

We evaluate our models against FLUXCOM-X-BASE as the state-of-the-art product, alongside three additional baselines:

- CT-LSTM:** a standard LSTM augmented with one-hot encoded static features;
- TAMLSTM:** the decoder-only component of TAM-RL;
- XGBoost:** trained on flattened (non-temporal) feature vectors, configured with the same hyperparameters as FLUXCOM-X-BASE for methodological consistency.

Each neural network model is represented as a mean ensemble over ten independently trained runs (different random seeds), ensuring comparability with XGBoost, which is ensemble-based by design. FLUXCOM-X-BASE provides hourly GPP and NEE estimates, which we averaged to daily values to match our models' output resolution, along with spatial resolution and grid alignment.

Models were trained on the site list used in FLUXCOM-X-BASE and evaluated on the remaining 164 held-out sites. Fig. 3 shows RMSE distributions across IGBP ecoregions and Köppen–Geiger climate zones, computed on highest-quality observations (NEE\_VUT\_USTAR50\_QC = 1); error bars reflect within-category variance across sites. Across the five dominant climate types, CT-LSTM, TAMLSTM, and TAM-RL consistently outperform XGBoost and FLUXCOM-X-BASE, though performance degrades for certain IGBP classes such as water bodies (WAT).

Fig. 4 presents a relative RMSE heatmap computed as  $(y_{fluxcom-x-base} - \hat{y})/y_{fluxcom-x-base}$ , offering a comparative rather than absolute view of improvement, with site and sample counts shown per IGBP type. Fig. 5 provides per-site RMSE and  $R^2$  comparisons between TAM-RL and FLUXCOM-X-BASE: points above the diagonal in the RMSE plot indicate improved accuracy, while points below the diagonal in the  $R^2$  plot indicate higher explained variance.

## Summary

Tab. 1 aggregates average performance metrics across all sites for each target and model. TAM-RL consistently achieves the lowest RMSE and highest  $R^2$  across both tar-

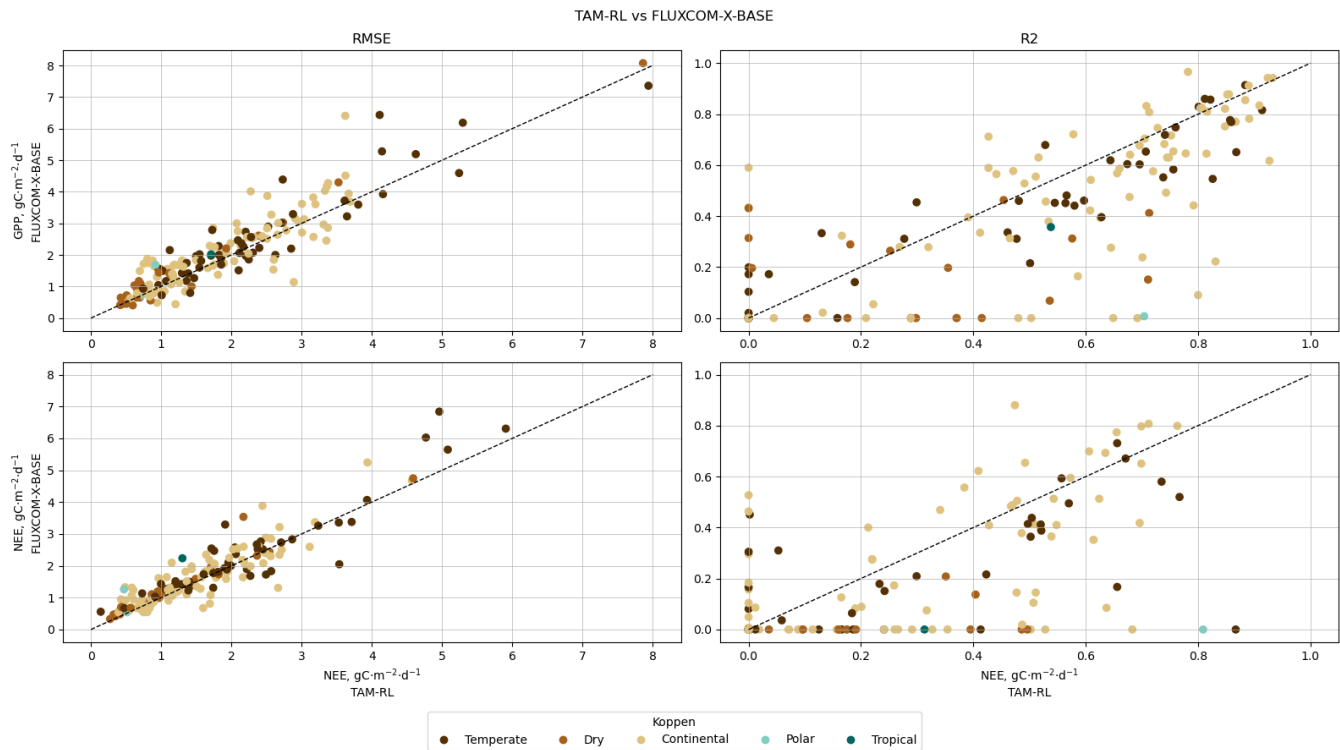


Figure 5: Scatter plots of RMSE and  $R^2$  of TAM-RL and FLUXCOM-X-BASE computed for every site and colored by the Köppen climate type.

Table 1: Model performance comparison across targets. Metrics are averaged across all sites. NEE\_VUT\_USTAR50\_QC=1 and NEE\_VUT\_REF\_QC=1.

Model	GPP		NEE	
	RMSE	$R^2$	RMSE	$R^2$
CT-LSTM	2.03	0.42	1.67	0.21
TAMLSTM	2.04	0.40	1.63	0.21
TAM-RL	<b>1.97</b>	<b>0.43</b>	<b>1.62</b>	<b>0.23</b>
XGBoost	2.17	0.34	1.76	0.16
FLUXCOM-X-BASE	2.18	0.36	1.76	0.16

gets: compared to FLUXCOM-X-BASE, our framework reduces RMSE by 9.6% for GPP and 8.0% for NEE, while improving  $R^2$  by 19.4% and 43.8%, respectively.

Several limitations remain. All models, including the XGBoost baseline, underperform on water bodies (WAT), suggesting the current feature set lacks variables capturing aquatic processes. A moderate performance drop is also observed for mixed forests (MF), deciduous broadleaf forests (DBF), and evergreen needleleaf forests (ENF), where RMSE differences relative to FLUXCOM-X-BASE range from 0.4–6.0% depending on the target.

More broadly, our analysis reveals substantial error variability across IGBP and Köppen–Geiger classes. While TAM-RL reduces this variance relative to baselines, spatial and climatic heterogeneity remain significant challenges for

reliable global carbon flux upscaling.

## Conclusion

We introduced TAM-RL, a task-aware representation learning framework for zero-shot upscaling terrestrial carbon fluxes, trained with a knowledge-guided composite loss. Across all experiments, TAM-RL on average outperforms FLUXCOM-X-BASE and conventional baselines, achieving lower RMSE and higher  $R^2$  for both GPP and NEE, while effectively capturing site-specific characteristics and temporal dynamics in the presence of sparse, heterogeneous EC data.

Challenges remain for underrepresented ecosystems, particularly water bodies and certain forest types, where performance lags behind, and substantial error variability persists across climate and ecoregion classes. Future work should focus on further developing methods for a better knowledge transfer between different locations as well as investigate variational or Bayesian extensions to better quantify and reduce predictive uncertainty in global carbon flux upscaling.

## References

Baldocchi, D.; Falge, E.; Gu, L.; Olson, R.; Hollinger, D.; Running, S.; Anthoni, P.; Bernhofer, C.; Davis, K.; Evans, R.; et al. 2001. FLUXNET: A new tool to study the temporal and spatial variability of ecosystem-scale carbon dioxide, water vapor, and energy flux densities. *Bulletin of the American Meteorological society*, 82(11): 2415–2434.

- Cai, S.; Wang, Z.; Wang, S.; Perdikaris, P.; and Karniadakis, G. E. 2021. Physics-informed neural networks for heat transfer problems. *Journal of Heat Transfer*, 143(6): 060801.
- Chen, T.; and Guestrin, C. 2016. Xgboost: A scalable tree boosting system. In *Proceedings of the 22nd acm sigkdd international conference on knowledge discovery and data mining*, 785–794.
- Cui, D.; Liang, S.; Wang, D.; and Liu, Z. 2021. A 1 km global dataset of historical (1979–2013) and future (2020–2100) Köppen–Geiger climate classification and bioclimatic variables. *Earth System Science Data*, 13(11): 5087–5114.
- Fan, B.; Zhang, H. K.; Li, Z. B.; Xiao, J.; Che, X.; Liu, Z.; Camps-Valls, G.; and Chen, J. M. 2025. Estimating carbon fluxes over North America using a physics-constrained deep learning model. *ISPRS Journal of Photogrammetry and Remote Sensing*, 227: 551–569.
- Friedl, M. A.; and Sulla-Menashe, D. 2019. MCD12Q1 MODIS/Terra+Aqua Land Cover Type Yearly L3 Global 500 m SIN Grid V006.
- Gorelick, N.; Hancher, M.; Dixon, M.; Ilyushchenko, S.; Thau, D.; and Moore, R. 2017. Google Earth Engine: Planetary-scale geospatial analysis for everyone. *Remote sensing of Environment*, 202: 18–27.
- Ji, W.; and Deng, S. 2021. Autonomous discovery of unknown reaction pathways from data by chemical reaction neural network. *The Journal of Physical Chemistry A*, 125(4): 1082–1092.
- Jung, M.; Schwalm, C.; Migliavacca, M.; Walther, S.; Camps-Valls, G.; Koirala, S.; Anthoni, P.; Besnard, S.; Bodesheim, P.; Carvalhais, N.; et al. 2020. Scaling carbon fluxes from eddy covariance sites to globe: synthesis and evaluation of the FLUXCOM approach. *Biogeosciences*, 17(5): 1343–1365.
- Karpatne, A.; Jia, X.; and Kumar, V. 2024. Knowledge-guided machine learning: Current trends and future prospects. *arXiv preprint arXiv:2403.15989*.
- Liu, L.; Zhou, W.; Guan, K.; Peng, B.; Xu, S.; Tang, J.; Zhu, Q.; Till, J.; Jia, X.; Jiang, C.; et al. 2024. Knowledge-guided machine learning can improve carbon cycle quantification in agroecosystems. *Nature communications*, 15(1): 357.
- Masson-Delmotte, V.; Zhai, P.; Pirani, A.; Connors, S. L.; Péan, C.; Berger, S.; Caud, N.; Chen, Y.; Goldfarb, L.; Gomis, M. I.; et al. 2021. Summary for policymakers.
- Muñoz-Sabater, J.; Dutra, E.; Agustí-Panareda, A.; Albergel, C.; Arduini, G.; Balsamo, G.; Boussetta, S.; Choulga, M.; Harrigan, S.; Hersbach, H.; et al. 2021. ERA5-Land: A state-of-the-art global reanalysis dataset for land applications. *Earth system science data*, 13(9): 4349–4383.
- Nathaniel, J.; Liu, J.; and Gentine, P. 2023. MetaFlux: Meta-learning global carbon fluxes from sparse spatiotemporal observations. *Scientific Data*, 10(1): 440.
- Nelson, J. A.; Walther, S.; Gans, F.; Kraft, B.; Weber, U.; Novick, K.; Buchmann, N.; Migliavacca, M.; Wohlfahrt, G.; Šigut, L.; et al. 2024. X-BASE: the first terrestrial carbon and water flux products from an extended data-driven scaling framework, FLUXCOM-X. *Biogeosciences*, 21(22): 5079–5115.
- Novick, K. A.; Biederman, J.; Desai, A.; Litvak, M.; Moore, D. J.; Scott, R.; and Torn, M. 2018. The AmeriFlux network: A coalition of the willing. *Agricultural and Forest Meteorology*, 249: 444–456.
- Pastorello, G.; Trotta, C.; Canfora, E.; Chu, H.; Christianson, D.; Cheah, Y.-W.; Poindexter, C.; Chen, J.; Elbashandy, A.; Humphrey, M.; et al. 2020. The FLUXNET2015 dataset and the ONEFlux processing pipeline for eddy covariance data. *Scientific data*, 7(1): 225.
- Read, J. S.; Jia, X.; Willard, J.; Appling, A. P.; Zwart, J. A.; Oliver, S. K.; Karpatne, A.; Hansen, G. J.; Hanson, P. C.; Watkins, W.; et al. 2019. Process-guided deep learning predictions of lake water temperature. *Water Resources Research*, 55(11): 9173–9190.
- Rebmann, C.; Aubinet, M.; Schmid, H.; Arriga, N.; Aurela, M.; Burba, G.; Clement, R.; De Ligne, A.; Fratini, G.; Gielen, B.; et al. 2018. ICOS eddy covariance flux-station site setup: a review. *International Agrophysics*, 32(4): 471–494.
- Ren, P.; Rao, C.; Liu, Y.; Wang, J.-X.; and Sun, H. 2022. PhyCRNet: Physics-informed convolutional-recurrent network for solving spatiotemporal PDEs. *Computer Methods in Applied Mechanics and Engineering*, 389: 114399.
- Renganathan, A.; Ghosh, R.; Khandelwal, A.; and Kumar, V. 2025. Task Aware Modulation using Representation Learning: An Approach for Few Shot Learning in Environmental Systems. In *Proceedings of the 2025 SIAM International Conference on Data Mining (SDM)*, 11–20. SIAM.
- Ueyama, M.; Takao, Y.; Yazawa, H.; Tanaka, M.; Yabuki, H.; Kumagai, T.; Iwata, H.; Awal, M. A.; Du, M.; Harazono, Y.; et al. 2025. The JapanFlux2024 dataset for eddy covariance observations covering Japan and East Asia from 1990 to 2023. *Earth System Science Data*, 17(8): 3807–3833.
- Vermote, E.; and Wolfe, R. 2015. MOD09GA MODIS/Terra Surface Reflectance Daily L2G Global 1 km and 500 m SIN Grid V006.
- Wu, Z.; Wang, H.; He, C.; Zhang, B.; Xu, T.; and Chen, Q. 2023. The application of physics-informed machine learning in multiphysics modeling in chemical engineering. *Industrial & Engineering Chemistry Research*, 62(44): 18178–18204.
- Xu, T.; and Valocchi, A. J. 2015. Data-driven methods to improve baseflow prediction of a regional groundwater model. *Computers & Geosciences*, 85: 124–136.
- Yuan, Q.; Wang, X.; Che, T.; and Li, J. 2025. Global carbon flux dataset generated by fusing remote sensing and multiple flux networks observation. *Scientific Data*, 12(1): 1359.